mice that showed defects in TLR3, TLR7 and TLR9 signalling, as well as Classes I and II MHC-restricted antigen presentation. The mutation was subsequently identified as a single histidine-to-arginine substitution (H412R) in the polytopic transmembrane protein UNC93B.

UNC93B is known to be essential for TLR3, TLR7 and TLR9 signalling in both humans and mice, and physically directs interactions with these TLRs to reach endolysosomes, where they bind ligands and initiate signalling [6–9]. The UNC93B gene is expressed in human DCs and B cells, but not T cells [10], and in the absence of UNC93B cells are unable to respond to TLR stimulation [9]. Moreover, with the exception of TLR3, triggering of all TLRs induces their recruitment to the intracytoplasmic domain of complexes formed with the adaptor protein myeloid differentiation factor 88 (MyD88) and IL-1 receptor-associated kinase-4 (IRAK-4), which mediate signalling of these receptors [10]. Interestingly, patients deficient in IRAK-4, MyD88 and UNC93B demonstrate an accumulation of autoreactive B cells expressing ANA, but do not display autoreactive antibodies in their serum or develop autoimmune disease [10].

In the current study, we examined the levels of IRAK-4, MyD88 and UNC93B expression on peripheral blood B cells isolated from patients with active SLE, and investigated any correlations with clinical parameters.

Patients and methods

Patients and clinical data assessments

We obtained peripheral blood from 43 active SLE patients, 20 inactive SLE patients (Table 1) and 40 healthy controls [age: 27.8 (3.5) mean (S.D.); male/female: 18/22]. All SLE patients fulfilled the 1997 revised criteria of the ACR [11]. We assessed clinical data including SLEDAI, serum levels of complement C3, C4, CH50 and anti-dsDNA antibody production using a RIA for each SLE patient. This study was approved by the ethics committee of Juntendo University and was undertaken in accordance with the principles outlined in the Declaration of Helsinki. Signed informed consent was obtained from all patients prior to the onset of the experiment.

Cell preparation and stimulation

Peripheral blood mononuclear cells (PBMCs) were isolated using Lymphoprep (Nycomed Pharma AS, Oslo, Norway) and collected at a concentration of 1×10^6 cells/ml. For B-cell isolation, B cells were labelled with anti-human CD20 antibody coupled with colloidal paramagnetic microbeads (Miltenyi Biotech, Bergisch-Gladbach, Germany) and isolated using AutoMACS (Miltenyi Biotech). Flow cytometric analysis revealed that B cells were isolated at a purity of >93%.

Isolated SLE B cells differentiated for 3 days were replated in 96-well round bottom plates at 1×10^5 cells/well. Cells were then stimulated with medium, oligodeoxynucleotides (ODNs) 2006 (5′-TCGTCGTTTTGTCGTTTTGTCGTT-3′), ODN2216 (5′-GGGGGACGATCGTCGGGGGG-3′) and ODN-TTAGGG (5′-TTTAGGGTTAGGGTTAGGGTTAGGG-3′) (Invivogen, San Diego, CA, USA), as described previously [4].

UNC93B mRNA analysis

Total RNA was isolated from 1×10^6 PBMCs, B cells and 1×10^5 stimulated B cells using the RNeasy Mini kit (Qiagen, Valencia, CA, USA). RT reactions were undertaken using the High Capacity cDNA Reverse Transcription Kit (Applied BioSystems, Foster City, CA, USA) according to the manufacturer's protocol. Quantitative RT–PCR (Q-PCR) was performed in a 25-μl reaction volume containing 12.5 μl of Power SYBR Green Master Mix (Applied BioSystems), 10 nM forward and reverse primers for UNC93B (5′-TGATCCTGCACTACGACGAG and 3′-GCGAGGAACATCATCCACTT), IRAK-4 (5′-GCAGGAATAGAAGATGAACAAA and 3′-GCTTCAAATCTCCTTATGTGAAACTG), MyD88 (5′-GCACATGGGCACATACAGAC and 3′-ACT

Table 1 Characteristics of patients

Characteristic	Active SLE patients ($n = 43$)	Inactive SLE patients ($n = 20$)
Age, mean (S.D.), years	34.7 (9.5)	34.9 (6.6)
Sex, males/females, *n*	19/24	9/11
Duration of SLE, mean (S.D.) years	5.15 (4.84)	5.14 (4.35)
SLEDAI, mean (S.D.) (range)	8.33 (4.75) (4–22)	2.85 (1.93) (0–3)
C3, mean (S.D.) (range) mg/dl	59.1 (26.4) (12–103)	87.8 (22.8) (53–144)
C4, mean (S.D.) (range) mg/dl	11.9 (8.86) (0–32)	16.9 (7.11) (4–30)
CH50, mean (S.D.) (range) U/ml	24.1 (14.1) (7–46)	35.2 (10.1) (14–48)
Anti-DNA antibody, mean (S.D.) (range) IU/ml	72.4 (75.2) (2.7–300)	7.93 (7.21) (0–30)
Prednisolone, *n* (%), mean dosage (mg/day)	25 (62.5), 11.47	13 (65) 7.92
Immunosuppressive therapy	0	2
Renal manifestation, *n* (%)	14 (35)	3 (15)
Arthritis, *n* (%)	17 (42.5)	4 (20)
Cytopenia, *n* (%)	10 (25)	1 (0.5)
CNS, *n* (%)	4 (10)	1 (0.5)
Cutaneous manifestation, *n* (%)	18 (45)	9 (45)
Serositis, *n* (%)	2 (5)	2 (1)

CCCTCGGATTGGTACAG) or β-actin (5′-GGACTTCGAGC AAGAGATG and 3′-AGCACTGTGTTGGCGTACA) and 1 μg of cDNA. The cycling conditions were 95°C for 10 min, followed by 40 cycles at 95°C for 15 s and 60°C for 1 min for denaturing and annealing–extension, respectively. UNC93B levels were measured on an ABI PRISM 7500 Sequence Detection System (Applied BioSystems). PCR products were separated on a 2% agarose gel and stained with ethidium bromide. UNC93B mRNA levels were normalized to β-actin for each sample.

Western blot analysis

B-cell whole-cell lysate (10 μl) was separated on 10% SDS–polyacrylamide gels and transferred to polyvinylidene difluoride membranes (Millipore, Billerica, MA, USA). Membranes were then blocked with blocking buffer containing phosphate-buffered saline–0.5% Tween-20 (PBS-T) and 3% skim milk for 90 min, and washed three times in 0.5% PBS-T. UNC93B protein was detected using rabbit anti-human UNC93B antibody (Imgenex, San Diego, CA, USA) diluted in blocking buffer (final concentration was 0.25 μg/ml) and incubated for 2 h at room temperature. The membrane was then incubated with a 1:5000 dilution of rabbit secondary alkali-phosphate antibody (Santa Cruz Biotechnology, San Diego, CA, USA) for 90 min. After three washes in 0.5% PBS-T, the membranes were stained with 5-Bromo-4-Chloro-3′-Indolylphosphatase p-Toluidine salt Table; Inactive SLE patients-Prednisolome/nitro-blue tetrazolium chloride (BCIP/NBT)/NBT solution (KPL, Gaithersburg, MD, USA).

Statistical analysis

Statistical analysis was performed using the Mann–Whitney U-test and Spearman's correlation coefficient. The results of the ODN-stimulated assay were analysed using the Kruskal–Wallis test and Sheffe's method. Statistical significance was defined as $P < 0.05$.

Results

Expression of UNC93B on SLE B cells

We initially examined the expression of UNC93B mRNA on PBMCs from SLE patients and healthy controls.

FIG. 1 Expression of UNC93B on B cells isolated from active SLE patients and healthy controls.

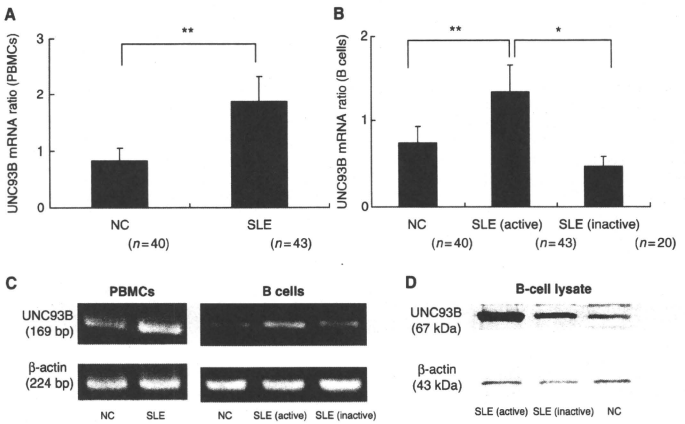

(A) Expression of UNC93B mRNA on PBMCs from SLE patients was significantly higher than normal controls (NC; $^{**}P = 0.0021$). **(B** and **C)** Expression of UNC93B mRNA on B cells from active SLE patients was significantly higher than NC ($^{**}P = 0.0042$) and inactive SLE patients ($^{*}P = 0.045$). UNC93B or β-actin samples (10 μl) were used as templates for RT–PCR. The products were separated on 2% Tris-borate-edta agarose gels containing 0.5 μg/ml ethidium bromide and visualized under UV. Error bars represent mean (S.D.) **(D)** Expression of UNC93B protein on B cells from active SLE patients was analysed by SDS–PAGE. For detection, membranes were stained with BCIP/NBT solution (KPL). **(E)** Significant correlation was found between UNC93B mRNA expression on B cells and anti-dsDNA antibody production ($P = 0.00002$, $R = 0.688$), **(F)** C3 levels ($P = 0.0002$, $R = -0.558$) or **(G)** the point of SLEDAI ($P = 0.00003$, $R = 0.651$) in active SLE patients. Serum anti-DNA antibody was analysed using RIA and the normal levels were found to be <2.0 IU/ml.

FIG. 1 Continued.

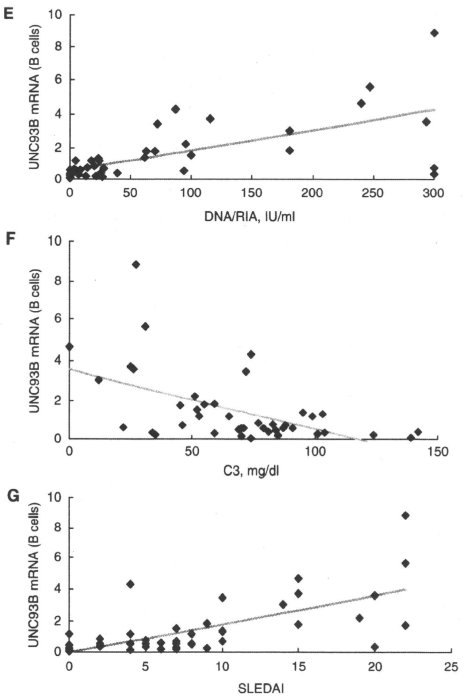

As shown in Fig. 1A, UNC93B mRNA on PBMCs from SLE patients was expressed at significantly higher levels than in the healthy controls ($P = 0.0021$).

We previously reported that high expression levels of TLR9 were present on the peripheral blood B cells derived from active SLE patients. Therefore, to assess whether the mechanisms underlying the production of autoreactive B cells involves TLR9, we next examined UNC93B mRNA and protein expression on B cells from lupus patients and healthy controls. The expression of UNC93B mRNA on $CD20^+$ B cells from active SLE patients was significantly higher than the healthy controls ($P = 0.0042$) and inactive patients ($P = 0.045$) (Fig. 1B and C). We also found that the intracellular expression of UNC93B protein in $CD20^+$ B cells from active SLE patients was higher than that in the healthy controls and inactive SLE (Fig. 1D). In contrast, the expression levels of IRAK-4 and MyD88 mRNA on B cells did not significantly differ between active SLE patients and healthy controls (supplementary figure 1, available as supplementary data at *Rheumatology* Online).

We next investigated whether TLR9–CpG interaction induced activation of UNC93B. We have previously shown that B cells isolated from active SLE patients express high levels of TLR9. Given these results, we stimulated active B cells from SLE patients with CpG ODN. As shown in supplementary figure 2 (available as supplementary data at *Rheumatology* Online), B cells stimulated with ODN2006 ($P = 0.0049$) and ODN2216 ($P = 0.045$) demonstrated enhanced expression of UNC93B mRNA.

Correlation with clinical data

We next investigated the relationship between UNC93B mRNA expression on B cells isolated from active SLE

patients and laboratory data (CH50, C3, C4 and titre of anti-dsDNA antibody). We found a significant correlation between UNC93B mRNA levels on B cells and anti-dsDNA antibody production (Fig. 1E, $P = 0.00002$, $R = 0.688$) or C3 (Fig. 1F, $P = 0.0002$, $R = -0.558$) or SLEDAI (Fig. 1G, $P = 0.00003$, $R = 0.651$) in active lupus patients.

Discussion

In the current study, we demonstrate that UNC93B mRNA expression levels in PBMCs and B cells isolated from active SLE patients were significantly higher than those in healthy controls and inactive SLE patients when assessed using Q-PCR and western blotting. We also show that the expression levels of IRAK-4 and MyD88 mRNA on B cells from SLE patients was not significantly higher than those in the healthy controls. Furthermore, the expression levels of UNC93B mRNA correlated significantly with the production of anti-dsDNA antibody or the amount of C3, or the point of SLEDAI in active SLE patients.

It is well established that the levels of intracellular TLRs including TLR7, TLR8 and TLR9 correlate with the pathogenesis of murine SLE, and that TLR9 in particular plays an essential role in the pathogenesis of murine lupus models [12]. In SLE patients, we have recently demonstrated that TLR9 present on the peripheral blood B cells is also associated with the pathogenesis of SLE [4]. More recently, some reports have suggested that TLR7 and TLR9 expression levels, and TLR9 levels on $CD19^+$ B cells from SLE patients, are significantly higher than those in healthy controls [13, 15]. In contrast, TLR3 expression does not appear to be up-regulated in human lupus [14, 15]. Thus, it is suggested that TLR7 and TLR9 may play a specific role in the pathogenesis of SLE.

Previous reports have demonstrated that UNC93B specifically controls trafficking of nucleotide-sensing TLRs, such as TLR7 and TLR9 [6]. Isnardi *et al.* [10] reported that signalling through IRAK-4 and MyD88 complexes plays a major role in the establishment of central B-cell tolerance in the bone marrow by counter-selecting developing autoreactive B cells including ANA-expressing cells. Moreover, they were able to show that UNC93B-deficient patients displayed an increased frequency of polyreactive new emigrant B cells [10]. As TLR3, TLR7, TLR8 and TLR9 are the only receptors that require functional UNC93B, and given that TLR3 signalling does not require IRAK-4 and MyD88 formation, it appears likely that TLR7, TLR8 and TLR9 are responsible for the removal of autoreactive B cells in the periphery [10]. Little is known about the cells and molecules that regulate human peripheral tolerance, and about how TLR7, TLR8 and TLR9 may be involved in these regulatory processes. Our recent data revealed that up-regulation of B cell activating factor of the TNF family (BAFF), which is known to be a B-cell survival factor present on SLE B cells, may prevent the removal of autoreactive B cells by increasing their survival in the periphery of SLE patients [16]. In addition, our current data showed that the expression levels of IRAK-4 and MyD88 mRNA on B cells from active SLE patients were not significantly greater than those in the healthy controls. We considered the possibilities that the UNC93B interacts directly with TLR9 and MyD88/IRAK4 signalling pathway triggered by not only TLR7, TLR8, TLR9 but also via TIR domain-containing adaptor protein (TIRAP) from TLR4, and another one is that it is more powerful with LPS-TLR4 signalling than with CpGdDNA-TLR9 signalling.

In conclusion, we report up-regulation of the ER membrane protein UNC93B on B cells in patients with active SLE and a significant correlation with the clinical data and disease activity. These data suggest that TLR9 signalling through UNC93B plays a partial role in the pathogenesis of SLE by preventing peripheral B-cell tolerance.

Rheumatology key messages

- UNC93B is present in intracellular B cells in active SLE patients.
- UNC93B mRNA correlated significantly with the levels of anti-dsDNA antibody present in SLE patients.
- Intracellular TLR and UNC93B play an essential role in SLE pathogenesis.

Acknowledgements

We are grateful to Jacinta Sagona and D. Douglas for assistance in preparing the manuscript.

Funding: This study was supported in part by the High Technology Research Center Grant from Ministry of Education, Culture, Sports, Science and Technology, Japan.

Disclosure statement: The authors have declared no conflicts of interest.

References

1 Chan OT, Madaio MP, Shlomchik MJ. The central and multiple roles of B cells in lupus pathogenesis. Immunol Rev 1999;169:107–21.

2 Fernandez-Gutierrez B, de Miguel S, Morado C, Hernandez-Garcia C, Banares A, Jover JA. Defective early T and T-dependent B cell activation in systemic lupus erythematosus. Lupus 1998;7:314–22.

3 Anders HJ. A Toll for lupus. Lupus 2005;14:417–22.

4 Nakano S, Morimoto S, Suzuki J *et al.* The role of pathogenic autoantibody production by Toll-like receptor 9 of B cells in active systemic lupus erythematosus. Rheumatology 2008;47:145–9.

5 Latz E, Schoenemeyer A, Visintin A *et al.* TLR9 signals after translocating from the ER to CpG DNA in the lysosome. Nat Immunol 2004;5:190–8.

6 Kim YM, Brinkmann MM, Paquet ME, Ploegh HL. UNC93B delivers nucleotide-sensing toll-like receptors to endolysosomes. Nature 2008;452:234–8.

7 Tabeta K, Hoebe K, Janssen EM *et al.* The UNC93B mutation 3d disrupts exogenous antigen presentation and signalling via Toll-like receptors 3, 7 and 9. Nat Immunol 2006;7:156–64.

8 Brinkmann MM, Spooner E, Hoebe K, Beutler B, Ploegh HL, Kim YM. The interaction between the ER membrane protein UNC93B and TLR3, 7, and 9 is crucial for TLR signalling. J Cell Biol 2007;177:265–75.

9 Casrouge A, Zhang SY, Eidenschenk C *et al.* Herpes simplex virus encephalitis in human UNC-93B deficiency. Science 2006;314:308–12.

10 Isnardi I, Ng YS, Srdanovic I *et al.* IRAK-4- and MyD88-dependent pathways are essential for the removal of developing autoreactive B cells in humans. Immunity 2008;29:746–57.

11 Hochberg MC. Updating the American College of Rheumatology revised criteria for the classification of systemic lupus erythematosus. Arthritis Rheum 1997;40:1725.

12 Christensen SR, Shupe J, Nickerson K *et al.* Toll-like receptor 7 and TLR9 dictate autoantibody specificity and have opposing inflammatory and regulatory roles in a murine model of lupus. Immunity 2006;25:417–28.

13 Komatsuda A, Wakui H, Iwamoto K *et al.* Up-regulated expression of Toll-like receptors mRNA in peripheral blood mononuclear cells from patients with systemic lupus erythematosus. Clin Exp Immunol 2008; 152:482–7.

14 Papadimitraki ED, Choulaki C, Koutala E *et al.* Expansion of Toll-like receptor 9-expressing B cells in active systemic lupus erythematosus. Arthritis Rheum 2006;54:3601–11.

15 Migita K, Miyashita T, Maeda Y *et al.* Toll-like receptor expression in lupus peripheral blood mononuclear cells. J Rheumatol 2007;34:493–500.

16 Morimoto S, Nakano S, Watanabe T *et al.* Expression of B-cell activating factor of the tumour necrosis factor family (BAFF) in T cells in active systemic lupus erythematosus: the role of BAFF in T cell-dependent B cell pathogenic autoantibody production. Rheumatology 2007;46:1083–6.

Biochemical and Biophysical Research Communications 394 (2010) 804–810

Contents lists available at ScienceDirect

Biochemical and Biophysical Research Communications

journal homepage: www.elsevier.com/locate/ybbrc

FTY720 exerts a survival advantage through the prevention of end-stage glomerular inflammation in lupus-prone BXSB mice

Seiichiro Ando [a,*], Hirofumi Amano [a], Eri Amano [a], Kentaro Minowa [a], Takashi Watanabe [a], Soichiro Nakano [a], Yutaka Nakiri [a], Shinji Morimoto [a], Yoshiaki Tokano [a], Qingshun Lin [b], Rong Hou [b], Mareki Ohtsuji [b], Hiromichi Tsurui [b], Sachiko Hirose [b], Yoshinari Takasaki [a]

[a] Department of Rheumatology and Internal Medicine, Juntendo University School of Medicine, 2-1-1 Hongo, Bunkyo-ku, Tokyo 113-8421, Japan
[b] Department of Pathology, Juntendo University School of Medicine, 2-1-1 Hongo, Bunkyo-ku, Tokyo 113-8421, Japan

ARTICLE INFO

Article history:
Received 3 March 2010
Available online 15 March 2010

Keywords:
Sphingosine 1-phosphate (S1P) receptors
FTY720
SLE
Lupus nephritis
BXSB mice

ABSTRACT

FTY720 is a novel investigational agent targeting the sphingosine 1-phosphate (S1P) receptors with an ability to cause immunosuppression by inducing lymphocyte sequestration in lymphoid organs. Systemic lupus erythematosus (SLE) is refractory autoimmune disease characterized by the production of a wide variety of autoantibodies and immune complex (IC)-mediated lupus nephritis. Among several SLE-prone strains of mice, BXSB is unique in terms of the disease-associated monocytosis in periphery and the reduced frequency of marginal zone B (MZ B) cells in spleen. In the present study, we examined the effect of FTY720 on lupus nephritis of BXSB mice. FTY720 treatment resulted in a marked decrease in lymphocytes, but not monocytes, in peripheral blood, and caused relocalization of marginal zone B (MZ B) cells into the follicle in the spleen. These changes did not affect the production of autoantibodies, thus IgG and C3 were deposited in glomeruli in FTY720-treated mice. Despite these IC depositions, FTY720-treated mice showed survival advantage with the improved proteinuria. Histological analysis revealed that FTY720 suppressed mesangial cell proliferation and inflammatory cell infiltration. These results suggest that FTY720 ameliorates lupus nephritis by inhibiting the end-stage inflammatory process following IC deposition in glomeruli.

1. Introduction

The FTY720 molecule is a synthetic analog of a natural product isolated from the filamentous fungus *Isaria sinclairii*, and causes immunosuppression by inducing lymphocyte retention in secondary lymphoid organs [1–3]. FTY720 has structural similarities to the lysophospholipid, and becomes phosphorylated *in vivo* by sphingosine kinases. Phosphorylated FTY720 acts as a high-affinity agonist for the sphingosine 1-phosphate (S1P) receptor on lymphocytes, inducing aberrant internalization of the receptor [4]. This renders the cells unresponsive to serum S1P, depriving them of a signal necessary for egress from lymphoid organs. Therefore it induces the sequestration of circulating mature lymphocytes into secondary lymphoid organs and thereby decreases the number of lymphocytes in peripheral blood [1]. FTY720 also modulates chemotactic responses and lymphocyte trafficking to divert lymphocytes from inflammatory lesions and graft sites [2]. So far, great potentials of FTY720 has been reported for the treatment of relapsing multiple sclerosis [5] and the prevention of kidney transplant rejection [6] in human clinical trials.

Systemic lupus erythematosus (SLE) is refractory autoimmune disease characterized by the production of a wide variety of autoantibodies and immune complex (IC)-mediated tissue inflammation. IC-type lupus nephritis is a common complication that significantly worsens mortality. Treatment with corticosteroids and various immunosuppressive agents may be useful in many cases; however, these drugs have an immunosuppressive effect on immune cell function and toxicity-related complications limit their long-term usage. Therefore, it is necessary to develop new treatment strategies. In this context, FTY720 is a possible alternative, since FTY720 exerts its immunosuppressive effect without impairing lymphocyte function. Trials for FTY720 treatment for SLE were carried out using SLE-prone MRL/*lpr* [7] and (NZB × NZW) F1 mice [8]. While each study demonstrated a therapeutic effect of FTY720 treatment, the underling mechanism may differ from each other. In MRL/*lpr* mice, FTY720 suppressed

Abbreviations: S1P, sphingosine 1-phosphate; SLE, systemic lupus erythematosus; IC, immune complex; MZ B cells, marginal zone B cells; Fo B cells, follicular B cells; PBL, peripheral blood leukocyte; MCP-1, monocyte chemoattractant protein-1; PAS, periodic acid-Schiff.

* Corresponding author. Fax: +81 3 5800 4893.
E-mail address: andosei78102@biscuit.ocn.ne.jp (S. Ando).

0006-291X/$ - see front matter © 2010 Elsevier Inc. All rights reserved.
doi:10.1016/j.bbrc.2010.03.078

autoantibody production in association with the marked decrease in splenic lymphocytes [7]. In contrast, FTY720 had no effect on autoantibody production and glomerular mesangial expansion, while proteinuria was greatly improved in FTY720-treated (NZB × NZW) F1 mice [8]. Thus, further studies are needed to thoroughly understand the FTY720-mediated suppressive effect on lupus nephritis.

The SLE-prone BXSB mice develop severe lupus nephritis in association with the production of various autoantibodies [9]. The disease is more severe in males than in females due to involvement of the Y chromosome-linked autoimmune acceleration (*Yaa*) mutation, which is a consequence of translocation of the telomeric segment of the X chromosome including the gene encoding Toll-like receptor 7 onto the Y chromosome [10,11]. Unique features in BXSB male mice are the disease-associated increase in monocytes in periphery [12], and the defect in the development of marginal zone B (MZ B) cells [13]. Intriguingly, it has been shown that the localization of B cells in the splenic white pulp is highly dependent on S1P receptor signals, and that FTY720 rapidly induces MZ B cell migration into follicles [14]. In the present study, we examined the effect of FTY720 on the lymphocyte localization and on the disease features in BXSB male mice.

2. Materials and methods

2.1. Mice and treatment

BXSB mice were purchased from the Shizuoka Laboratory Animal Center, Shizuoka, Japan. Three-month-old BXSB male mice were given *per os* FTY720 (1 mg/kg in distilled water) or distilled water alone three times a week for 5 months. FTY720 was generously provided by Mitsubishi Tanabe Pharma Corporation (Osaka, Japan). All mice were housed under identical conditions, and all experiments were performed in accordance with our institutional guidelines. Only male mice were analyzed.

2.2. Cell count and flow cytometric analysis

Peripheral blood leukocyte (PBL) counts were analyzed using automated counter SF-3000 (Sysmex Co., Kobe, Japan) according to the manufacturers' instruction. Spleen cells or PBL were stained with the following mAbs: FITC-conjugated anti-CD4, -B220, -CD69, -CD21, and -CD1d mAbs, PE-conjugated anti-CD8, -CD138, -CD11a (anti-αL integrin subunit), -CD69, -CD18 (anti-β2 integrin subunit), and -CD21 mAbs, APC-conjugated anti-B220 mAb, and biotin-conjugated anti-CD23, and -CD11b mAbs, followed by avidin-PE/Cy5 or avidin-APC/Cy7. All reagents were obtained from BD PharMingen (San Jose, California). Stained cells were analyzed using a FACScan flow cytometer and WinMDI software ver. 2.8 (Joseph Trotter).

2.3. Estimation of proteinuria

The severity of renal disease was monitored by biweekly measurement of proteinuria, using Albustix (Bayer Medical Ltd., Tokyo). Proteinuria was scored from grade 0 to 4, according to the amount of urinary albumin, in which $1 \geq 30$ mg/100 ml, $2 \geq 100$ mg/100 ml, $3 \geq 300$ mg/100 ml, and $4 \geq 1000$ mg/100 ml. Mice with levels over grade 3 in repeated tests were considered to be positive for proteinuria.

2.4. Serum levels of anti-DNA antibodies

Anti-DNA antibodies of IgM and IgG classes were determined by ELISA, using ELISA plates coated with dsDNA prepared from calf thymus. Binding activities were expressed in units, referring to a standard curve obtained by serial dilution of a standard serum pool from NZB mice over 6 months of age for IgM class antibodies and (NZB x NZW) F1 mice over 8 months of age for IgG class antibodies, respectively. Both contain 1000 U activities/ml.

2.5. Histopathology and tissue immunofluorescence

Tissues were fixed in 4% paraformaldehyde, embedded in paraffin, cut into sections 4 μm thick and stained with periodic acid-Schiff (PAS) hematoxylin solution. For immunohistochemical analysis, frozen kidney sections were stained with FITC-conjugated goat antibodies against IgG or C3 (ICN Pharmaceuticals, Inc., Aurora, OH). The extent of IgG and C3 deposition in glomeruli was evaluated by measurement of relative fluorescence signal intensity per pixel in each glomerular area in total 20–25 randomly selected glomeruli from three individual mice of each control and FTY720-treated group. To analyze cell infiltration in the kidney, three color staining was performed using digoxygenin-conjugated anti-F4/80, Alexa488-conjugated anti-CD4, and Alexa546-conjugated anti-CD8 mAbs, followed by Cy5-conjugated anti-digoxygenin antibody. Since it is difficult to count absolute cell number of infiltrated macrophages, the extent of $F4/80^+$ macrophage infiltration was evaluated by summing anti-F4/80 mAb-mediated relative fluorescence signal intensity of each pixel in each glomerular area in total 185 and 136 glomeruli including Bowman's capsule from three individual mice in control and FTY720-treated mice, respectively. The extent of $CD4^+$ and $CD8^+$ T cell infiltration was evaluated by cell counting in each glomerular area. For analysis of splenic tissues, frozen sections were stained with FITC-conjugated anti-CD1d and Alexa546-conjugated anti-MAdCAM1 mAbs. Color images were obtained using laser scanning microscopy.

2.6. Quantitative real-time RT-PCR analysis of MCP-1 transcripts

Total RNA was isolated from kidney and first-strand cDNA was synthesized using an oligo (dT) primer. The MCP-1 gene was amplified with forward primer (5′-AGGTCCCTGTCATGCTTCTG-3′) and reverse primer (5′-TCTGGACCCATTCCTTCTTG-3′). A reference control gene (β-actin) was amplified with forward primer (5′-AGCC ATGTACGTAGCCATCC-3′) and reverse primer (5′-CTCTCAGCTGTGG TGGTGAA-3′) to standardize amounts of RNA and allow calculation of relative amounts of MCP-1 expression, using a GeneAmp 5700 Sequence Detection system (ABI). The PCR primers for MCP-1 and β-actin were designed according to published sequences in MGI database (MCP-1, NM_011333; β-actin, NM_ 007393).

2.7. Statistics

Statistical analysis of survival rate and the incidence of proteinuria were done using log-rank test and Fisher's exact test, respectively. Differences in frequencies of leukocyte subsets, serum levels of antibodies and relative MCP-1 expression level were analyzed by Mann–Whitney *U* test. The extent of IC deposition in glomeruli, and macrophage/T-cell infiltration in kidney was compared using *z* test. Differences at $P < 0.05$ were considered to be statistically significant.

3. Results

3.1. Effects of FTY720 on the clinical course of BXSB lupus

To confirm the effect of FTY720, numbers of PBL were examined one month after the treatment (Fig. 1A). In control vehicle-treated mice, major population was composed of $B220^+$ B cells and $CD11b^+$ monocytes, and numbers of $CD4^+$ and $CD8^+$ T cells were small. In

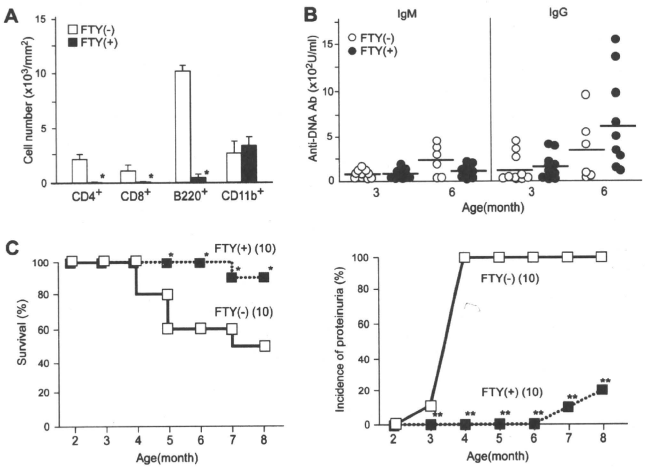

Fig. 1. Effects of FTY720 on clinical course of BXSB male mice. (A) Comparisons of cell numbers of $CD4^+$ T cells, $CD8^+$ T cells, $B220^+$ B cells, and $CD11b^+$ monocytes in peripheral blood one month after the beginning of treatment between control vehicle-treated and FTY720-treated BXSB male mice. Mean and SE of six mice in each group are shown. Asterisk indicates statistically significant difference between two groups of mice ($P < 0.05$). (B) Comparisons of serum levels of IgM and IgG anti-DNA antibodies between two groups of mice at 3 and 6 months of age. Horizontal bar represents the mean level. There was no significant difference in antibody levels between two groups of mice. (C) Comparisons of survival rate and cumulative incidence of proteinuria between two groups of mice. The numbers of mice examined are shown in parentheses. Asterisk indicates statistically significant difference ($P < 0.05$, $P < 0.0005$).

FTY720-treated mice, $CD4^+$ and $CD8^+$ T cells almost disappeared and $B220^+$ B cells dramatically decreased, thus indicating the significant effect on lymphocyte depletion in peripheral blood. In contrast, there was no difference in number of $CD11b^+$ monocytes between two groups of mice.

We then compared the serum levels of anti-DNA antibodies. The result showed that there was no significant difference in antibody levels of both IgM and IgG classes between control and FTY720-treated mice at 3 and 6 months of age (Fig. 1B). Fig. 1C compares the survival rate and the cumulative incidence of proteinuria. Five out of 10 control mice (50%) died at 7 months of age; however, 9 out of 10 FTY720-treated mice (90%) were still alive at that time. As for the proteinuria, while all of 10 control mice (100%) were positive at 4 months of age onward, the onset of proteinuria was markedly delayed in the FTY720-treated mice and only two out of 10 mice (20%) were positive even at 8 months of age.

3.2. Effects of FTY720 on histopathological changes in lupus nephritis

Histopathological and immunofluorescence findings in the glomeruli were compared between 6-month-old control and FTY720-treated mice (Fig. 2A). In control mice, glomeruli were enlarged, and mesangial cell proliferation and thickening of glomerular capillary walls along with deposition of PAS-positive materials, including IgG and complement component C3, were prominent. In contrast, glomeruli in FTY720-treated mice were normal in size and showed no mesangial cell proliferation. Intriguingly, however, a considerable amount of IgG and C3 was deposited mainly in mesangial area. When comparing the extent of IgG and C3 deposition in glomeruli by evaluating relative fluorescence signal intensity per pixel, there was no significant difference between two groups of mice (Fig. 2B).

We then examined the extent of inflammatory cell infiltration in the kidney. As shown in Fig. 2C, there were abundant $F4/80^+$ macrophages and some $CD4^+$ T and $CD8^+$ T cells infiltrated around the glomeruli in control mice. When evaluating the extent of macrophage infiltration by summing anti-F4/80 mAb-mediated relative fluorescence intensity in each glomerular area, macrophage infiltration was significantly reduced in FTY720-treated mice. It was also evident that the number of $CD4^+$ T cells infiltrated in each glomerular area was significantly decreased by FTY720 treatment. Quantitative real-time RT-PCR revealed that mRNA expression level of monocyte chemoattractant protein (MCP)-1, a major chemoattractant for monocyte/macrophage migration [15], was significantly reduced in FTY720-treated mice (Fig. 2D).

3.3. Effects of FTY720 on spleen cell subsets

FTY720 showed no effect on splenomegaly, a characteristic feature in BXSB mice, and there was no significant difference in spleen weight between two groups of mice at 6 months of age (Table 1). We then examined spleen cell subsets using flow cytometric analysis. While there was no significant difference in the frequencies of $CD4^+$ T cells, $CD8^+$ T cells, $B220^+$ B cells, $CD138^+$ plasma cells, and $CD11b^+$ macrophages per total cells between the two groups of mice, frequencies of activated cells expressing CD69 antigen tended to be higher in FTY720-treated mice and the difference in frequency of $CD69^+CD4^+$ T cells per total CD4 T cells was statistically significant (Table 1). These findings suggest that FTY720 induces the sequestration of circulating activated lymphocytes into spleen.

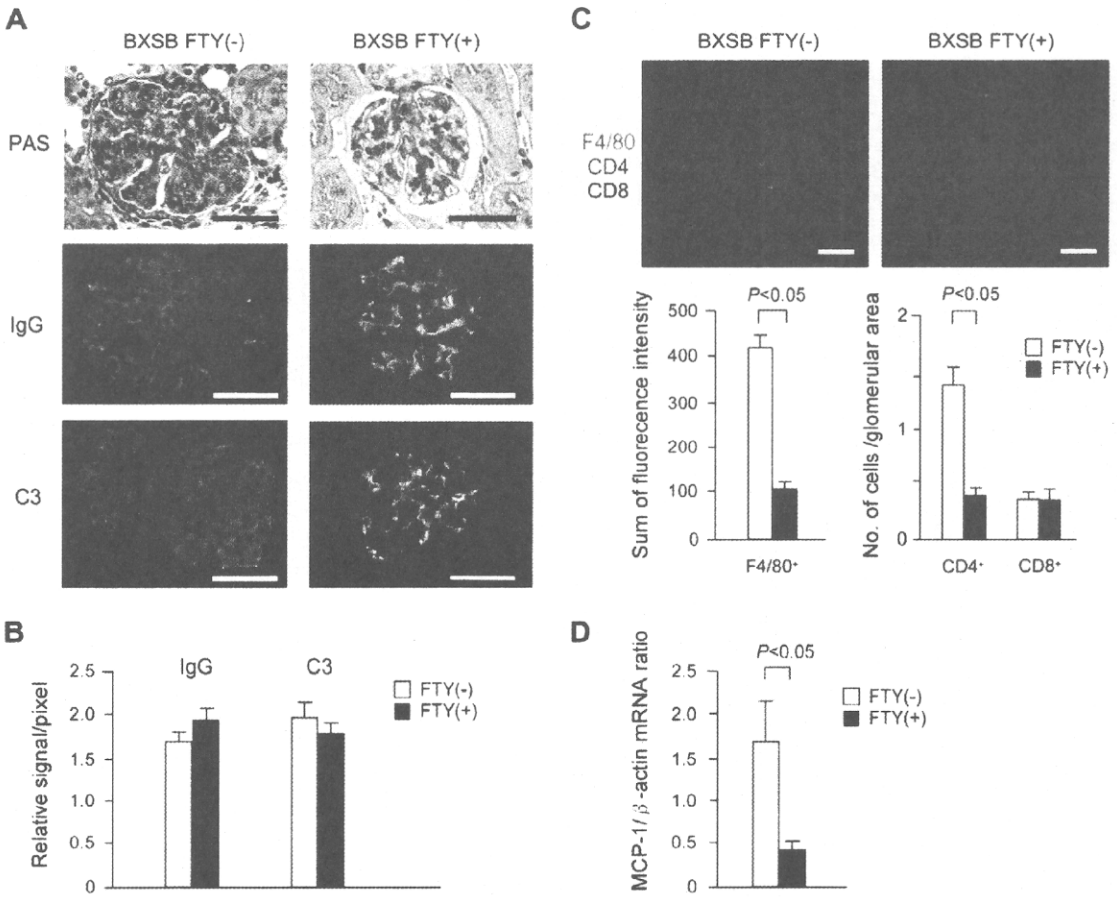

Fig. 2. Comparisons of renal pathology and MCP-1 mRNA expression level in kidney between control vehicle-treated and FTY720-treated BXSB male mice at 6 months of age. (A) Histological (PAS) and immunohistochemical findings for deposition of IgG and C3. The bar represents 50 μm. Representative result obtained from six mice of each strain is shown. (B) Comparisons of the extent of IgG and C3 deposition in glomeruli between two groups of mice. Mean and SE of relative fluorescence signal per pixel were shown (for details, see Section 2). (C) Immunohistochemical examination of infiltration of F4/80$^+$ macrophages, CD4$^+$ T cells and CD8$^+$ T cells in the kidney. The bar represents 50 μm. Representative result obtained from three mice in each strain is shown. Statistical analysis is shown for the difference in extent of F4/80$^+$ macrophage infiltration, estimated by summing anti-F4/80 mAb-mediated fluorescence intensity (for details, see Section 2), and of the difference in number of CD4$^+$ and CD8$^+$ T cells infiltrated in each glomerular area between the two groups of mice. Mean and SE are shown with the statistics. (D) Quantitative real-time RT-PCR analysis of MCP-1 mRNA expression in kidney samples obtained from five individual mice in each group. Mean and SE of relative expression of MCP-1 (MCP-1/β-actin ratio) are shown with the statistics.

Table 1
Effects of FTY720 on spleen weight and frequencies of splenic cell subsets.[a]

	BXSB FTY(−) (n = 5)	BXSB FTY(+) (n = 6)
Spleen weight (g)	0.44 ± 0.11	0.31 ± 0.05
CD4$^+$ T/total cells	15.5 ± 2.9	13.1 ± 1.7
CD69$^+$CD4$^+$ T/total CD4$^+$ T	28.8 ± 7.1	48.3 ± 6.9*
CD8$^+$ T/total cells	4.1 ± 0.7	3.2 ± 0.3
CD69$^+$CD8$^+$ T/total CD8$^+$ T	15.4 ± 3.1	20.0 ± 5.8
B220$^+$ B/total cells	40.1 ± 3.4	42.7 ± 5.9
CD69$^+$B220$^+$ B/total B	11.6 ± 1.7	14.2 ± 2.8
CD138$^+$ plasma/total cells	3.4 ± 1.0	5.4 ± 1.2
CD11b$^+$ macrophages/total cells	26.6 ± 3.6	32.2 ± 7.6

[a] Results were obtained at 6 months of age and shown with the mean ± SE.
* Difference in frequency between two groups of mice was statistically significant (P < 0.01).

We then examined the effect of FTY720 on splenic B-cell subsets at 4 and 6 months of age. As shown in Fig. 3A, flow cytometric analysis revealed that the frequency of CD21^{hi}CD23^{lo}B220$^+$ MZ B-cell subset per total B220$^+$ B cells was low in control mice, consistent with our previous report [13]. In contrast, the frequency of this subset was increased in process of FTY720 treatment, and this difference became statistically significant at 6 months of age. At this age, frequency of CD21^{int}CD23^{hi}B220$^+$ follicular B (Fo B)-cell subset was contrarily decreased in FTY720-treated mice. We next examined whether the increased MZ B-cell subset in FTY720-treated mice carries other characteristic MZ B-cell phenotypes, such as high expression levels of CD1d, αL and β2 integrin subunits [16]. In both control and FTY720-treated mice, the expression levels of these molecules in the gated CD21^{hi}CD23^{lo}B220$^+$ MZ B-cell subset were higher than those in the gated CD21^{int}CD23^{hi}B220$^+$ Fo B-cell subset (Fig. 3B).

To examine the effect of FTY720 treatment on MZ B-cell localization, immunohistochemical studies were done using antibodies against CD1d and MAdCAM1. As shown in Fig. 3C, cells with CD1d^{hi} MZ B-cell phenotype were scarcely observed in control mice, while, in FTY720-treated mice, these cells increased in some degree at 4 months of age and accumulated at 6 months of age in the follicles of the white pulp.

4. Discussion

The present study provided evidence that long-term treatment with FTY720 suppress end-stage lupus nephritis, but was not able to suppress autoantibody production and IC deposition in renal glomeruli. It has been shown that FTY720 may induce apoptosis

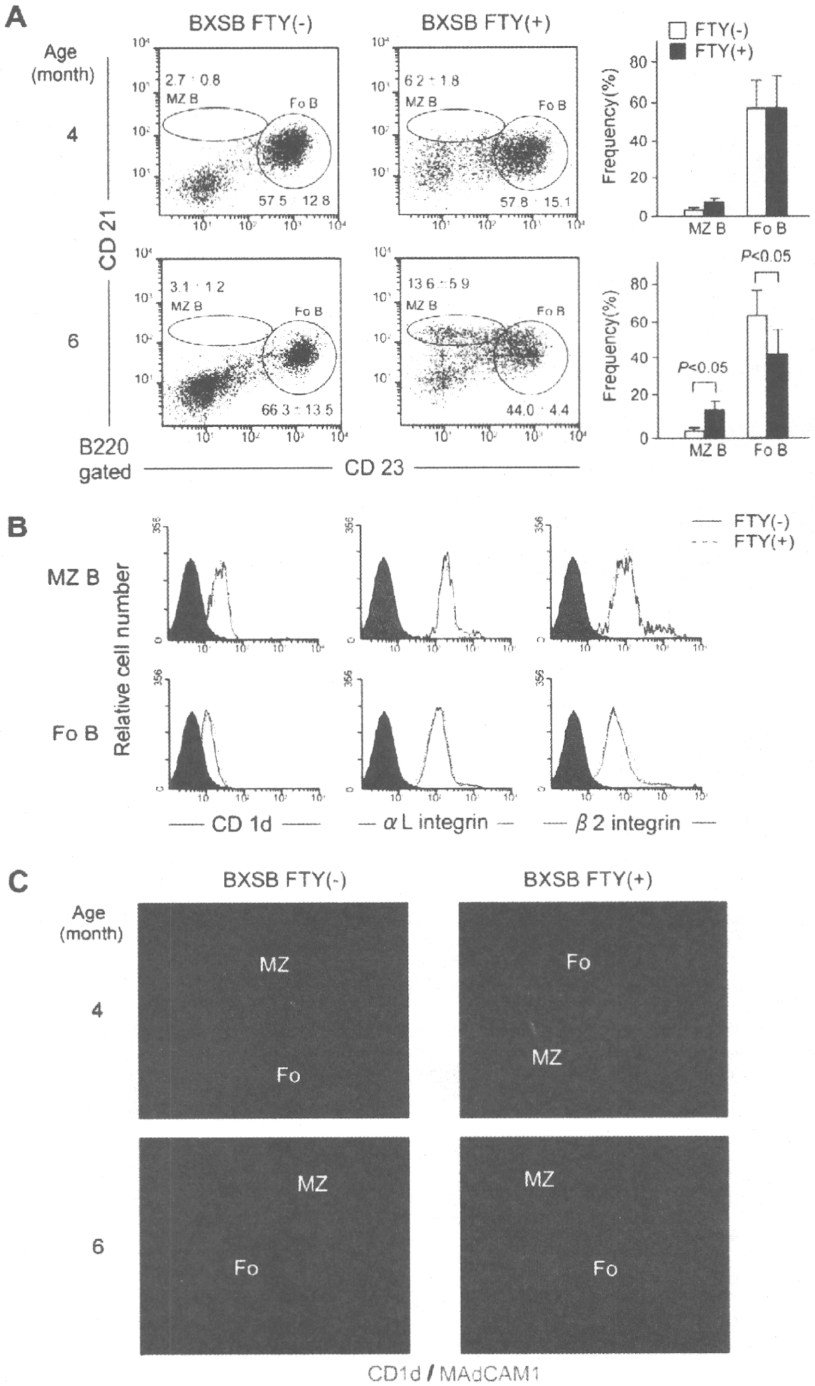

Fig. 3. Effect of FTY720 on splenic B-cell subsets. (A) Comparisons of flow cytometric profiles of splenic B cell-subsets between control vehicle-treated and FTY720-treated BXSB male mice at 4 and 6 months of age. The percentages of $CD21^{hi}CD23^{lo}B220^{+}$ MZ B cells and $CD21^{int}CD23^{hi}B220^{+}$ Fo B cells per B220-gated total B cells are shown. Representative profile obtained from six mice in each group is shown. The frequency of MZ B cells and Fo B cells in FTY720-treated BXSB mice was significantly higher and lower, respectively, than in control mice at 6 months of age. (B) Comparisons of expression levels of CD1d, αL, and β2 integrin subunits in MZ B and Fo B cells between two groups of mice. Closed areas indicate background staining. Representative result obtained from five mice aged 6 months in each group is shown. (C) Frozen spleen sections from mice aged 4 and 6 months were two-color stained with mAbs against CD1d and MAdCAM1. Representative result obtained from six mice of each strain is shown. MZ, marginal zone; Fo, follicle.

in splenic lymphocyte, thus suppress spleen weight and autoantibody production in MRL/*lpr* mice [7]. However, this is not the case in the present study, since FTY720 showed no effect on not only spleen weight but also autoantibody production. The key mechanism for disease suppression is rather linked to the marked inhibition of mesangial cell proliferation and of infiltration of macrophages and $CD4^{+}$ T cells around the glomeruli, irrespective of the IC deposition in glomeruli. FTY720-treated BXSB male mice

showed considerably delayed onset and a low incidence of proteinuria and survived for a longer time, in comparison with control mice.

FTY720 treatment induced marked lymphopenia; however, there was no effect on monocyte count. This discrepancy between lymphocytes and monocytes seems to be due to the difference in mechanisms involved in migration from peripheral blood into secondary lymphoid organs between lymphocytes and monocytes. In this context, the report documenting that monocyte recruitment depends on MCP-1 is noteworthy [15]. Like lymphocytes, monocyte-derived macrophages express S1P receptor [17]; however, the expression level of S1P receptors on macrophages was not changed by FTY720 treatment [18], in contrast to the situation in lymphocytes. Thus, S1P receptor internalization and down-modulation by FTY720 may be differently regulated in a cell type-specific manner, and the marked reduction of macrophage infiltration in inflamed tissue of FTY720-treated mice may not be simply explained by down-modulation of S1P receptor expression. Since MCP-1 is a major chemoattractant for monocyte/macrophage migration [15] and MCP-1 expression level was significantly reduced in the kidney of FTY720-treated mice, it is possible that FTY720-induced reduction of macrophage infiltration may be due to reduced MCP-1 production by mesangial cells, the major producers of MCP-1 in glomerulonephritis [19].

The lack of kidney damage irrespective of IgG IC deposition in glomeruli observed in the present study has been also reported in IgG Fc receptor common γ chain-deficient (NZB $\times$ NZW) F1 [20] and BXSB male mice [21]. This uncoupling was shown to be due to blockade of Fc receptor activation on circulation leukocytes [22]. In the current study, the different mechanism may be responsible, because the activating Fc receptors are intact. Since S1P is abundantly stored in platelets [23] and stimulates mesangial cells through S1P receptors [24], it is possible to speculate that large amounts of S1P released from IC-activated platelets stimulate mesangial cells to produce several cytokines and chemokines, including MCP-1. Subsequently infiltrated macrophages may be activated by ICs deposited in glomeruli and then induce mesangial cell proliferation, as indicated by adoptive transfer experiment of macrophages [25]. We hypothesize that FTY720 treatment may down-modulate S1P receptor expression on mesangial cells, thereby inhibit S1P receptor-mediated mesangial cell stimulation to produce MCP-1, and subsequent macrophage infiltration and mesangial cell proliferation. However, further studies are needed to clarify the exact mechanism responsible for the uncoupling of IC deposition and kidney damage in the present study.

BXSB male mice uniquely show marked depletion of MZ B cells [13]; however, FTY720-treated mice showed the increase in the B-cell subset bearing the $CD1d^{hi}CD21^{hi}CD23^{lo}B220^{+}$ MZ B-cell phenotype located inside the follicle, but not in the marginal zone. It has been demonstrated that integrins play a critical role in the localization and retention of MZ B cells [16]. However, the observed relocalization of MZ B cells into the follicle may be due to the FTY720-induced down-modulation of S1P receptors as described [14], but not by the contribution of integrins, since the expression levels of αL and β integrin subunits in MZ B and Fo B cells in FTY720-treated BXSB mice were not different from those in the control mice. The increase in relocalized MZ B cells is likely due to the long-term treatment with FTY720, which may induce the accumulation of small population of MZ B cells, which may otherwise migrate into periphery. The lack of correlation between autoantibody production and the increase in relocalized MZ B cells seems to suggest that MZ B cells do not play a major role in autoantibody production in BXSB mice. Alternatively, one can not deny the possibility that MZ B cells have potential to produce autoantibodies and that these cell migrate from spleen into periphery in control BXSB mice, but relocalize and accumulate inside the follicle of splenic white pulp in FTY720-treated BXSB mice. It is well recognized that MZ B-phenotype cells produce IgM, but not IgG, class autoantibodies. Thus, the origin of IgG autoantibody in BXSB mice is still remains to be determined.

S1P is one of the several biologically active lysophospholipids that have been shown to induce a wide array of physiological and pathophysiological responses, including cellular differentiation, proliferation, migration, extracellular matrix deposition, and chemotactic responses [26]. Thus, a more thorough understanding of the mechanism responsible for FTY720-mediated disease suppression may clarify the role played by S1P in the pathogenesis of IC-mediated lupus nephritis and related diseases.

Acknowledgments

We thank Naoki Ishihara, Naomi Ohtsuji, and Keiko Nishikawa for excellent technical help.

References

[1] K. Chiba, Y. Yanagawa, Y. Masubuchi, H. Kataoka, T. Kawaguchi, M. Ohtsuki, Y. Hoshino, FTY720, a novel immunosuppressant, induces sequestration of circulating mature lymphocytes by acceleration of lymphocyte homing in rats. I. FTY720 selectively decreases the number of circulating mature lymphocytes by acceleration of lymphocyte homing, J. Immunol. 160 (1998) 5037–5044.

[2] V. Brinkmann, K.R. Lynch, FTY720: targeting G-protein-coupled receptors for sphingosine 1-phosphate in transplantation and autoimmunity, Curr. Opin. Immunol. 14 (2002) 569–575.

[3] H. Rosen, G. Sanna, C. Alfonso, Egress: a receptor-regulated step in lymphocyte trafficking, Immunol. Rev. 195 (2003) 160–177.

[4] M.H. Graler, E.J. Goetzl, The immunosuppressant FTY720 down-regulates sphingosine 1-phosphate G-protein-coupled receptors, FASEB J. 18 (2004) 551–553.

[5] L. Kappos, J. Antel, G. Comi, X. Montalban, P. O'Connor, C.H. Polman, T. Haas, A.A. Korn, G. Karlsson, E.W. Radue, Oral fingolimod (FTY720) for relapsing multiple sclerosis, N. Engl. J. Med. 355 (2006) 1124–1140.

[6] K. Budde, R.L. Schmouder, R. Brunkhorst, B. Nashan, P.W. Lucker, T. Mayer, S. Choudhury, A. Skerjanec, G. Kraus, H.H. Neumayer, First human trial of FTY720. A novel immunomodulator, in stable renal transplant patients, J. Am. Soc. Nephrol. 13 (2002) 1073–1083.

[7] H. Okazaki, D. Hirata, T. Kamimura, H. Sato, M. Iwamoto, T. Yoshio, J. Masuyama, A. Fujimura, E. Kobayashi, S. Kano, S. Minota, Effects of FTY720 in MRL-lpr/lpr mice: therapeutic potential in systemic lupus erythematosus, J. Rheumatol. 29 (2002) 707–716.

[8] G. Alperovich, I. Rama, N. Lloberas, M. Franquesa, R. Poveda, M. Goma, I. Herrero-Fresneda, J.M. Cruzado, N. Bolanos, M. Carrera, J.M. Grinyo, J. Torras, New immunosuppressor strategies in the treatment of murine lupus nephritis, Lupus 16 (2007) 18–24.

[9] B.S. Andrews, R.A. Eisenberg, A.N. Theofilopoulos, S. Izui, C.B. Wilson, P.J. McConahey, E.D. Murphy, J.B. Roths, F.J. Dixon, Spontaneous murine lupus-like syndromes. Clinical and immunopathological manifestations in several strains, J. Exp. Med. 148 (1978) 1198–1215.

[10] P. Pisitkun, J.A. Deane, M.J. Difilippantonio, T. Tarasenko, A.B. Satterthwaite, S. Bolland, Autoreactive B cell responses to RNA-related antigens due to TLR7 gene duplication, Science 312 (2006) 1669–1672.

[11] S. Subramanian, K. Tus, Q.Z. Li, A. Wang, X.H. Tian, J. Zhou, C. Liang, G. Bartov, L.D. McDaniel, X.J. Zhou, R.A. Schultz, E.K. Wakeland, A Tlr7 translocation accelerates systemic autoimmunity in murine lupus, Proc. Natl. Acad. Sci. USA 103 (2006) 9970–9975.

[12] D. Wofsy, C.E. Kerger, W.E. Seaman, Monocytosis in the BXSB model for systemic lupus erythematosus, J. Exp. Med. 159 (1984) 629–634.

[13] H. Amano, E. Amano, T. Moll, D. Marinkovic, N. Ibnou-Zekri, E. Martinez-Soria, I. Semac, T. Wirth, L. Nitschke, S. Izui, The Yaa mutation promoting murine lupus causes defective development of marginal zone B cells, J. Immunol. 170 (2003) 2293–2301.

[14] G. Cinamon, M. Matloubian, M.J. Lesneski, Y. Xu, C. Low, T. Lu, R.L. Proia, J.G. Cyster, Sphingosine 1-phosphate receptor 1 promotes B cell localization in the splenic marginal zone, Nat. Immunol. 5 (2004) 713–720.

[15] R.T. Palframan, S. Jung, G. Cheng, W. Weninger, Y. Luo, M. Dorf, D.R. Littman, B.J. Rollins, H. Zweerink, A. Rot, U.H. von Andrian, Inflammatory chemokine transport and presentation in HEV: a remote control mechanism for monocyte recruitment to lymph nodes in inflamed tissues, J. Exp. Med. 194 (2001) 1361–1373.

[16] T.T. Lu, J.G. Cyster, Integrin-mediated long-term B cell retention in the splenic marginal zone, Science 297 (2002) 409–412.

[17] H. Rosen, E.J. Goetzl, Sphingosine 1-phosphate and its receptors: an autocrine and paracrine network, Nat. Rev. Immunol. 5 (2005) 560–570.
[18] I.I. Singer, M. Tian, L.A. Wickham, J. Lin, S.S. Matheravidathu, M.J. Forrest, S. Mandala, E.J. Quackenbush, Sphingosine-1-phosphate agonists increase macrophage homing, lymphocyte contacts, and endothelial junctional complex formation in murine lymph nodes, J. Immunol. 175 (2005) 7151–7161.
[19] K. Hora, J.A. Satriano, A. Santiago, T. Mori, E.R. Stanley, Z. Shan, D. Schlondorff, Receptors for IgG complexes activate synthesis of monocyte chemoattractant peptide 1 and colony-stimulating factor 1, Proc. Natl. Acad. Sci. USA 89 (1992) 1745–1749.
[20] R. Clynes, C. Dumitru, J.V. Ravetch, Uncoupling of immune complex formation and kidney damage in autoimmune glomerulonephritis, Science 279 (1998) 1052–1054.
[21] Q. Lin, Y. Xiu, Y. Jiang, H. Tsurui, K. Nakamura, S. Kodera, M. Ohtsuji, N. Ohtsuji, W. Shiroiwa, K. Tsukamoto, H. Amano, E. Amano, K. Kinoshita, K. Sudo, H. Nishimura, S. Izui, T. Shirai, S. Hirose, Genetic dissection of the effects of stimulatory and inhibitory IgG Fc receptors on murine lupus, J. Immunol. 177 (2006) 1646–1654.
[22] A. Bergtold, A. Gavhane, V. D'Agati, M. Madaio, R. Clynes, FcR-bearing myeloid cells are responsible for triggering murine nephritis, J. Immunol. 177 (2006) 7287–7295.
[23] Y. Yatomi, Y. Igarashi, L. Yang, N. Hisano, R. Qi, N. Asazuma, K. Satoh, Y. Ozaki, S. Kume, Sphingosine 1-phosphate, a bioactive sphingolipid abundantly stored in platelets, is a normal constituent of human plasma and serum, J. Biochem. 121 (1997) 969–973.
[24] N. Hanafusa, Y. Yatomi, K. Yamada, Y. Hori, M. Nangaku, T. Okuda, T. Fujita, K. Kurokawa, M. Fukagawa, Sphingosine 1-phosphate stimulates rat mesangial cell proliferation from outside the cells, Nephrol. Dial. Transplant. 17 (2002) 580–586.
[25] Y. Ikezumi, L.A. Hurst, T. Masaki, R.C. Atkins, D.J. Nikolic-Paterson, Adoptive transfer studies demonstrate that macrophages can induce proteinuria and mesangial cell proliferation, Kidney Int. 63 (2003) 83–95.
[26] V.S. Kamanna, B.V. Bassa, S.H. Ganji, D.D. Roh, Bioactive lysophospholipids and mesangial cell intracellular signaling pathways: role in the pathobiology of kidney disease, Histol. Histopathol. 20 (2005) 603–613.

Toyama *et al. Arthritis Research & Therapy* 2010, **12**:R92
http://arthritis-research.com/content/12/3/R92

arthritis research&therapy

RESEARCH ARTICLE Open Access

Inhibitory effects of ZSTK474, a novel phosphoinositide 3-kinase inhibitor, on osteoclasts and collagen-induced arthritis in mice

Shoko Toyama[1], Naoto Tamura*[1], Kazuhiko Haruta[2], Takeo Karakida[3], Shigeyuki Mori[2], Tetsuo Watanabe[2], Takao Yamori[4] and Yoshinari Takasaki[1]

Abstract

Introduction: Targeting joint destruction induced by osteoclasts (OCs) is critical for management of patients with rheumatoid arthritis (RA). Since phosphoinositide 3-kinase (PI3-K) plays a critical role in osteoclastogenesis and bone resorption, we examined the effects of ZSTK474, a novel phosphoinositide 3-kinase (PI3-K)-specific inhibitor, on murine OCs *in vitro* and *in vivo*.

Methods: The inhibitory effect of ZSTK474 on OC formation was determined and compared with other PI3-K inhibitors by counting tartrate-resistant acid phosphatase (TRAP)-positive multinucleated cells after culturing murine bone marrow monocytic OC precursors, and RAW264.7 cells. Activation of Akt and expression of nuclear factor of activated T cells (NFAT) c1 in cultured RAW264.7 cells were examined. The suppressing effect of ZSTK474 on bone resorption was assessed by the pit formation assay. The *in vivo* effects of ZSTK474 were studied in collagen-induced arthritis (CIA) in the mouse. Oral daily administration of ZSTK474 was started either when more than half or when all mice developed arthritis. Effects of ZSTK474 were evaluated using the arthritis score and histological score of the hind paws.

Results: ZSTK474 inhibited the differentiation of bone marrow OC precursors and RAW264.7 cells in a dose-dependent manner. The inhibitory effect of ZSTK474 was much stronger than that of LY294002, the most commonly used PI3-K inhibitor. In addition, ZSTK474 suppressed the bone resorbing activity of mature OCs. Moreover, oral daily administration of ZSTK474, even when begun after the development of arthritis, ameliorated CIA in mice without apparent toxicity. Histological examination of the hind paw demonstrated noticeable reduction of inflammation and of cartilage destruction in ZSTK474-treated mice. ZSTK474 also significantly decreased OC formation adjacent to the tarsal bone of the hind paw.

Conclusions: These findings suggest that inhibition of PI3-K with ZSTK474 may potentially suppress synovial inflammation and bone destruction in patients with RA.

Introduction

Rheumatoid arthritis (RA) is a systemic autoimmune disease characterized by chronic inflammation of the synovium as well as by destruction of inflamed joints through bone erosion. The management of patients with RA consists of both reduction of inflammation and protection of the joints from structural damage [1]. Some anti-rheumatic drugs, including biologics, are quite useful but are not effective in all patients; hence, new therapeutic agents are required.

It has been speculated that joint destruction is directly caused by osteoclasts (OCs) [2], which differentiate from monocytic precursors that have infiltrated the inflamed joints. After this infiltration, monocytic precursors convert to tartrate -resistant acid phosphatase (TRAP)-positive cells and fuse with each other, eventually forming giant multinucleated OCs. Although the growth and differentiation of OCs mainly depend on receptor activator of nuclear factor κB ligand (RANKL) and macrophage-colony stimulating factor (M-CSF), proinflammatory

* Correspondence: tnaoto@juntendo.ac.jp
[1] Department of Internal Medicine and Rheumatology, Juntendo University School of Medicine, 2-1-1 Hongo, Bunkyo-ku, Tokyo, 113-8421, Japan
Full list of author information is available at the end of the article

cytokines, such as tumor necrosis factor (TNF)-α, which are over-expressed in the inflamed joints, promote this process [3]. After differentiation, αvβ3 integrins on differentiated OCs engage with the bone extracellular matrix; this process is followed by bone resorption [4,5]. It has been demonstrated that this increased resorbing activity of OCs results not only in bone erosion and further joint destruction but also in systemic osteoporosis in patients with RA. Therefore, suppressing OCs is a major aspect of RA therapy [6,7].

Signal transduction via the phosphoinositide 3-kinase (PI3-K)/Akt pathway is essential for regulating cellular responses, such as proliferation, survival, migration, motility and tumorigenesis, in a variety of cell types [8], not just OCs. Class I PI3-Ks are heterodimers and are found in four isoforms. Class IA PI3-Ks (PI3-Kα, PI3-Kβ and PI3-Kδ) are composed of a catalytic subunit p110 (α, β, or δ) and a regulatory subunit p85 (α or β), and activated through tyrosine kinase signaling. The class IB PI3-K (PI3-Kγ) is a heterodimer consisting of a catalytic subunit p110γ associated with one of two regulatory subunits, p101 and p84, and activated via seven-transmembrane G-protein-coupled receptors (GPCRs) [9]. Whereas the expression of PI3-Kα and PI3-Kβ is ubiquitous, that of PI3-Kδ and PI3-Kγ is mainly restricted to hematopoietic cells [8].

Many signal transduction molecules are involved in different phases of growth and development in OCs, such as Src homology-2 (SH2)-containing inositol-5-phosphatase (SHIP), Vav3, Gab2, extracellular signal-regulated kinase (ERK) and p38 mitogen-activated protein kinase (MAPK) [10-14]. In OCs, PI3-K is a major downstream effecter of the M-CSF receptor, RANK, and αβv3 integrin. The importance of PI3-K for differentiation, survival and motility of OCs has been demonstrated by using the PI3-K inhibitors wortmannin and LY294002 [15-22], and also by studying mice deficient in the expression of the p85α subunit of class IA PI3-K [23]. In addition, several transcription factors, including NF-kB, c-fos, AP-1, PU.1, and CREB, are involved in regulating osteoclastogenesis in its early or late phase, and expression of NFATc1 is specific to the RANKL induced-signaling pathway and essential for terminal differentiation of OCs [24,25].

Wortmannin and LY294002, potent inhibitors of PI3-K that have been extensively used for studying *ex vivo* PI3-K-driven signal pathways, also inhibit other related enzymes [9,26]. LY294002 causes severe dermal toxicity [27], and wortmannin and its analog has shown hepatic toxicity [28] when administered in mice. ZSTK474, a synthesized *s*-triazine derivative that strongly inhibited the growth of tumor cells, was subsequently identified as a novel PI3-K-specific inhibitor [29-33]. Furthermore, ZSTK474 is suitable for oral administration, and demonstrated marked *in vivo* antitumor activity in mice grafted with human cancer cells without showing toxicity to major organs [29].

Since the action of ZSTK474 on OCs is unknown, we examined the effects of ZSTK474 in an *in vitro* OC culture system and found strong inhibitory effects on the differentiation and bone resorbing activity of OCs. Moreover, daily administration of ZSTK474 ameliorated collagen-induced arthritis (CIA) in mice, remarkably reducing the migration of inflammatory cells and OCs in the synovial tissue.

Materials and methods

PI3-K inhibitors

ZSTK474 and IC87114 (a PI3-Kδ-selective inhibitor) were synthesized at Central Research Laboratories of Zenyaku Kogyo Co. Ltd. (Tokyo Japan). LY294002 was purchased from Sigma Chemical Co. (St Louis, MO, USA). AS605240 (a PI3-Kδ-selective inhibitor) was purchased from Calbiochem (Schwalbach, Germany). In *in vivo* experiments, ZSTK474 was prepared as a solid dispersion [34].

Animals

Male DBA/1 mice (eight weeks old) were purchased from Charles River Laboratories Japan (Kanagawa, Japan). They were maintained at approximately 22°C with a 12-hour light/dark cycle and given standard chow and tap water *ad libitum*. Newborn ddY mice were obtained from the Japan SLC, Inc. (Shizuoka, Japan). All animal experiments were approved by the local ethical committees of each institution.

Osteloclast formation

In vitro OC formation was examined as previously described [35]. Briefly, primary osteoblasts derived from growing calvarial cells of newborn ddY mice at three- to four-days of age were suspended in alpha-minimum essential medium (α-MEM, Sigma) supplemented with 10% (v/v) fetal bovine serum (FBS, Gibco BRL, Gaithersburg, MD, USA), 100 U/ml penicillin and 100 μg/ml streptomycin, and plated at a density of 2×10^4 cells/well in 24-well plates (Corning Incorporated, Corning, NY, USA) overnight. Mouse bone marrow cells containing monocytic OC precursors were removed aseptically from the tibiae of four- to six-week old ddY male mice, and co-cultured on adherent osteoblasts at a density of 1.0×10^6cells/well in medium containing 10^{-7} M 1α,25-$(OH)_2D_3$ (Wako Pure Chemical Industries, Ltd., Osaka, Japan) for five to six days in the presence or absence of varying concentrations of ZSTK474 or other PI3-K inhibitors. Otherwise, non-adherent bone marrow cells were cultured alone with 10 ng/ml of M-CSF (R & D Systems, Minneapolis, MN, USA) for two days, and then adherent cells were cultured with 100 ng/ml of soluble RANKL

(sRANKL) (R & D Systems) for three days. In some experiments, RAW264.7 cells (American Type Culture Collection, Manassas, VA, USA) were plated at a density of 2.5 × 10^4 cells/well in a 24-well tissue culture plate overnight, and sRANKL (100 ng/ml), TNF-α (50 ng/ml) and ZSTK474 were added. The medium was changed every two to three days. The cells were fixed with 3.7% formalin, permeabilized with 0.1% Triton X-100, and stained with TRAP. OC formation was determined by counting TRAP-positive multinucleated cells having three or more nuclei, and OCs were counted in each set of duplicated wells.

Real time-polymerase chain reaction (PCR) for the quantification of RANKL expression

The osteoblasts were plated at a density of 2 × 10^5 cells/well in six-well plates, and cultured with or without 1α,25-$(OH)_2D_3$ for 24 hours in the presence or absence of ZSTK474. Total RNA was extracted using a total RNA isolation kit (Ambion Inc., Austin. TX, USA), and 3 μg of the total RNA was reverse transcribed using a You-prime Fast-Strand Breads kit (Amersham Pharmacia Biotech, Inc., Piscataway, NJ, USA). The primers used in PCR were 5'-GACTCGACTCTGGAGAGT-3' (sense primer) and 5'-GAGAACTTGGGATTTTGATGC-3' (antisense primer) for RANKL and 5'-AGCCATGTACGTAGCCA-TCC (sense primer) and 3'-CTCTCAGCTGTGGTGGT-GAA (antisense primer) for β-actin. Real-time PCR was performed using 1 μg of cDNA and Power SYBR Green Master Mix (Applied Bio Systems, Foster City, CA, USA) on an ABI PRISM 7500 Sequence Detection System (Applied Bio Systems) with conditions at 95°C for 10 minutes, followed by 40 cycles at 95°C for 15 seconds and 60°C for one minute. The expression of RANKL was quantified using the comparative C_T, applying the formula $X_n = 2^{-\Delta CT}$, where X_n is the relative amount of target gene in question and ΔC_T is the difference between the C_T of the house keeping gene for a given sample [36].

Western blotting for Akt and NFATc1

RAW264.7 cells were plated at a density of 2.5 × 10^5 cells/well in a six-well tissue culture plate overnight, and ZSTK474 was added. After incubation for 30 minutes, 50 to 100 ng/ml of sRANKL, or sRANKL plus TNF-α (50 ng/ml), was added and the cells were incubated for the indicated time. Cells were washed twice with ice-cold phosphate-buffered saline (PBS) containing 1% phosphatase inhibitor cocktail (Sigma), detached with a cell scraper, centrifuged, and lysed with lysis buffer (1% Triton X-100, 1% phosphatase inhibitor cocktail and 1 mM of PMSF in Tris-buffer, pH 7.6). The lysates were boiled with sodium dodecyl sulfate (SDS) -sample buffer and run on SDS-PAGE followed by blotting with a 1:1000 dilution of anti-phospholylated Akt (anti-phospho Akt), anti-Akt, anti-IκB, anti-phospho cJun, anti-phospho p42/p44, anti-β-actin (Cell Signal Technology, Inc., Beverly, MA, USA) and anti-NFAT1c monoclonal antibody (Santa Cruz Biotechnology, Santa Cruz, CA, USA).

Immunofluorescence microscopy

RAW264.7 cells (200 μl, 2.5 × 10^5/ml) were plated onto Lab Tek Chamber slide (Thermo Fisher Scientific, Rochester, NY, USA) overnight. After treatment with 0.1 μM of ZSTK474 for 30 minutes, 100 ng/ml of sRANKL and 50 mg/ml of TNF-α were added, and the cells were cultured for 48 hours. Then, the cells were fixed with 4% paraformaldehyde, washed with PBS three times, permeabilized with 0.1% Triton X-100 in PBS, and blocked with 10% normal goat serum (Nichrei, Tokyo, Japan). The cells were incubated with anti-NFATc1 antibody diluted in PBS (1:50) for one hour, washed with PBS, and followed with phycoerythrin-conjugated goat anti-rabbit IgM+IgG (H+L chain specific, Beckman Coulter) for another one hour. The cells were postfixed in Aqua-Poly/Mount (Polysciences, Washington, PA, USA) and viewed using fluorescence microscope (Nikon ECLIPSE E600/Y-FL).

Bone resorbing activity of OC

A 10 cm culture dish (Corning) was coated with 5 ml of type I collagen mixture at 4°C. The dish was placed in a CO_2 incubator at 37°C for 10 minutes to render the aqueous type I collagen gelatinous. Primary osteoblasts (5 × 10^5 cells/dish) and bone marrow cells (6 × 10^6 cells/dish) were co-cultured on the collagen gel-coated dish for five days. The dish was then treated with 4 ml of 0.2% collagenase solution (Nitta Gelatin Co., Osaka, Japan) for 20 minutes at 37°C in a shaking water bath (60 cycles/minute). The cells were collected by centrifugation at 600 rpm for three minutes, then washed and suspended with α-MEM containing 10% FBS (OC preparation). Dentine slices (Immunodiagnostic Systems, Ltd., Boldon, UK) were cleaned by ultrasonication in distilled water, sterilized using 70% ethanol, dried under ultraviolet light, and placed in 96-well plates. A 0.1-ml aliquot of the OC preparation was transferred onto the slices. After incubation for 72 hours in the presence or absence of the PI3-K inhibitors, the medium was removed and 1 ml of 1 M NH_4OH was added to each well and incubated for 30 minutes. The dentin slices were then cleaned by ultrasonication, stained with hematoxylin (Wako Pure Chemical Industries) for 35 to 45 seconds, and washed with distilled water. The area of resorption pits that formed on dentine slices was observed under a light microscope and measured.

CIA in mice

Male DBA/1 mice, eight-weeks of age, were injected intradermally in the base of the tail with 200 μg of bovine type II collagen (Collagen Gijutsu Kenshu-Kai., Tokyo, Japan) emulsified in complete Freund's adjuvant (Difco, Detroit, MI, USA) on Day 1, and the same amount of the antigen emulsified in incomplete Freund's adjuvant (Difco) on Day 22. When half of the mice had developed arthritis (Day 28), the mice were randomly divided into four groups of eight mice. Each group orally received vehicle or 25, 50, 100 mg/kg of ZSTK474, once/day. In another therapeutic protocol, 100 mg/kg of ZSTK474 was administered from the day when all mice developed arthritis (Day 31). Total arthritis score was defined as the sum of the paw swelling scores for each paw (0 to 4 per paw), with a maximum score of 16. In the semi-therapeutic protocol, the mice were killed on Day 50, and the right hind paws were removed, fixed in paraformaldehyde, decalcified in Kalkitox (Wako Pure Chemical Industries, Ltd.), embedded in paraffin and sectioned. The sections were then stained with hematoxylin and eosin (H&E) or safranin O to assess hyperplasia of synovial tissue, infiltration of leukocytes, and destruction of cartilage. Each parameter was graded separately and assigned a severity score as follows: grade 0, no detectable change: 1 to 4, slight to severe changes. The number of OC in talus was counted in every third 6 μm section. To examine *in vivo* OC formation in CIA mice, the hind paws were removed on Day 52 and rapidly frozen in the therapeutic protocol. The frozen tissue was sectioned according to the method described previously [37] and the sections were stained with H&E or TRAP. Plasma TRACP5b levels were measured using a mouse TRAP™ Assay (Immunodiagnostic System Ltd).

Statistical analysis

Statistical significance of differences was assessed by one-way analysis of variance (ANOVA) followed by Dunnett's test or the Student's *t*-test for comparison of two samples. Statistical tests were performed using Kaleida graph 3.6 (Synergy Software, Reading, PA, USA). In all analyses, $P < 0.05$ was considered statistically significant.

Results

Inhibitory effects of ZSTK474 on OC formation in co-culture system

To determine whether ZSTK474 could inhibit osteoclastogenesis *in vitro*, mouse bone marrow monocytic precursors were co-cultured with osteoblasts together with $1\alpha,25\text{-}(OH)_2D_3$ in the presence or absence of various concentrations of ZSTK474 or other PI3-K inhibitors. The effect was also examined in OC differentiation of the bone marrow precursors in response to M-CSF and sRANKL. OC formation was significantly inhibited by ZSTK474 in both culture systems, and this inhibitory effect was much stronger than that of LY294002 (Figure 1a), the most commonly used PI3-K inhibitor at present. IC87114 also inhibited OC formation similarly to LY294002, whereas AS605240 had virtually no effect on the OC differentiation, indicating that PI3-Kδ might play a more important role in OC formation in these culture systems. ZSTK474 suppressed OC formation in a dose-dependent manner at lower concentrations (Figure 1b and 1c). No TRAP-positive cells were observed with 0.2 μM of ZSTK474, suggesting that differentiation of OCs was completely suppressed at this concentration. On the other hand, 0.04 μM of ZSTK474 were likely to allow the monocytic precursors to differentiate into small TRAP-positive cells, but not to form large OCs (Figure 1b). In addition, ZSTK474, even at 1 μM, did not decrease the expression of RANKL mRNA in osteoblasts cultured with $1\alpha,25\text{-}(OH)_2D_3$ (Figure 1d), indicating that RANKL expression on osteoblasts might not be involved in suppressing effect of ZSTK474 on OC differentiation.

Inhibition of Akt phosphorylation and NFATc1 expression in RAW264.7 cells by ZSTK474

To confirm that ZSTK474 affected the monocytic precursors but not the osteoblasts, we examined its effect on the phosphorylation of Akt in RAW264.7 cells. Phosphorylation of Akt induced by sRANKL (100 ng/ml) was abolished by ZSTK474 (Figure 2a). However, ZSTK474 did not inhibit the degradation of IκB and phosophorylation of JNK and ERK1/2 induced by sRANKL. On the other hand, the expression of NFATc1, which occurs in the late phase of OC differentiation and promotes terminal osteoclastogenesis in association with a complex of cJun and cFos [38,39], was attenuated in RAW264.7 cells treated with sRANKL by 0.1 μM of ZSTK474, although ZSTK474 did not apparently affect the expression of cFos (Figure 2b). We further analyzed translocation of NFATc1 by immunofluorescence microscopy. Calcium entry to OC precursor cells activates the calcium/calmodulin-dependent pathway, leading to NFATc1 translocation into the nucleus. ZSTK474 repressed the translocation of NFATc1 to the nucleus in response to sRANKL and TNF-α (Figure 2c). These results indicated that ZSTK474 at least blocked the RANK/RANKL-PI3-K/Akt cascade in monocytic precursors, resulting in inhibition of OC differentiation.

Inhibitory effects of ZSTK474 on OC formation induced by both RANKL and TNF-α

We next examined the effects of ZSTK474 on OC formation induced by RANKL and TNF-α, since it was speculated that TNF-α enhanced OC formation in RA. In fact, RANKL-induced phosphorylation of Akt was enhanced by the addition of TNF-α (Figure 2d). ZSTK474 (0.03, 0.1,

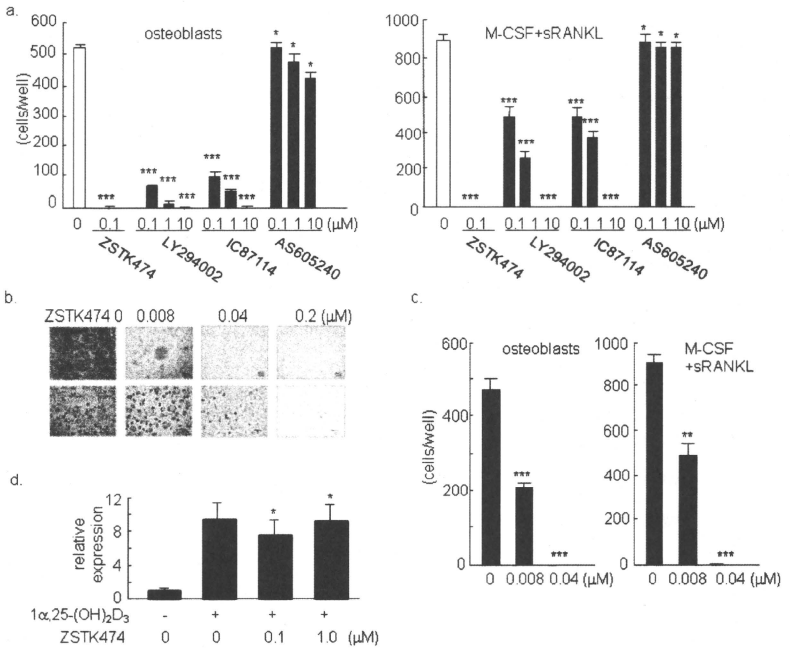

Figure 1 Inhibitory effect of ZSTK474 on OC formation. Mouse bone marrow cells containing OC precursors were cultured with osteoblasts in the presence of 1α,25-$(OH)_2D_3$ for five days. Indicated concentrations of ZSTK474, LY294002, AS605240 (a PI3-Kγ-selective inhibitor), or IC87114 (a PI3-Kδ-selective inhibitor) were added at the initiation of cultures. Mouse bone marrow cells were also cultured with M-CSF (10 ng/ml) for two days and then with M-CSF and sRANKL (100 ng/ml) for another three days. The inhibitors were added simultaneously with sRANKL. **a)** and **c)** TRAP-positive multinucleated cells were counted as OC. The columns and bars indicate the mean and standard deviation (S.D.) from duplicated wells. **b)** OC formation in co-culture with osteoblast (upper) and culture with M-CSF and sRANKL (lower). Representative results were shown in a, b, and c. **d)** RANKL mRNA was measured using real-time PCR, with results normalized the value of β-actin. The columns and bars indicate the mean and S.D. of three independent experiments. * = P > 0.05, ** = P < 0.01, *** = P < 0.001.

and 0.3 μM) inhibited the phosphorylation of Akt induced by RANKL (100 ng/ml) and TNF-α (50 ng/ml) in RAW264.7 cells (Figure 2d). Moreover, the OC formation induced by RANKL (100 ng/ml) and TNF-α (50 ng/ml) was inhibited by ZSTK474 in a dose-dependent manner. OC formation was completely inhibited by ZSTK474 (0.3 μM, Figure 2e).

Inhibition of bone resorbing activity of OC by ZSTK474

We next examined whether ZSTK474 also inhibited the bone-resorbing activity of mature OCs. The OCs that had matured on the collagen-gel were transferred onto dentine slices, the total areas of the resorbed pits were measured after three days culture. This experiment revealed that 0.1 μM of ZSTK474 completely prevented pit formation by OCs (Figure 3a, b). LY294002 and IC87114, but not AS605240, also inhibited the bone resorption more weakly (Figure 3b). Because PI3-K is important for OC survival [19], it was supposed that PI3-K inhibited the survival of mature OCs and consequently suppressed the bone resorption. Therefore, we tested whether ZSTK474 affected the survival of mature OCs. Complete and partial inhibition of OC survival was observed in the presence of 1 μM and 0.1 μM of ZSTK474, respectively (Figure 3c).

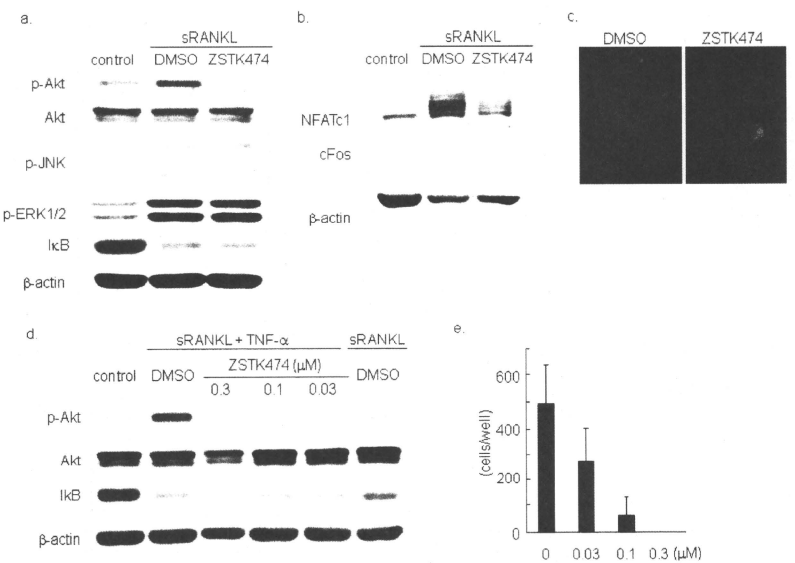

Figure 2 Suppressive effect of ZSTK474 on OC precursor cells. a) Inhibition of Akt phosphorylation by ZSTK474. RAW264.7 cells were incubated with or without 0.1 μM of ZSTK474 for 30 minutes and for another 15 minutes in the presence of soluble RANKL. The phosphorylated Alt (p-Akt) and whole Akt (Akt) were examined by the Western blotting. **b)** The expression of NFATc1 was determined in RAW264.7 cells cultured for 48 hours in the presence of soluble RANKL with or without ZSTK474 pretreatment. **c)** NFATc1 localization was visualized using immunofluorescence microscopy in RAW264.7 cells cultured with sRANKL and TNF-α for 24 hours. Treated with vehicle (left) and 0.1 μM of ZSTK474 (right). **d)** The phosphorylation of Akt in RAW264.7 cells cultured with soluble RANKL and TNF-α was inhibited by ZSTK474. **e)** RAW264.7 cells were cultured in the presence of RANKL and TNF-α in the presence or absence of ZSTK474. The number of TRAP staining-positive multinucleated cells was counted.

Amelioration of CIA in mice with oral administration of ZSTK474

To determine whether interference with PI3-K activity by ZSTK474 reduces joint destruction *in vivo*, we examined the effects of ZSTK474 on CIA in mice. ZSTK474 was administered from the day when more than 50% of the mice developed arthritis (Day 28). While vehicle-treated mice developed active arthritis, administration of daily oral ZSTK474 ameliorated joint inflammation in a dose-dependent manner. The arthritis score reached 7.5 ± 0.9 by Day 50 in the vehicle-treated group, whereas oral administration of ZSTK474 reduced the arthritis score to 4.1 ± 1.2 (25 mg/kg, $P < 0.05$), 1.3 ± 0.6 (50 mg/kg, $P < 0.001$), and 0.5 ± 0.5 (100 mg/kg, $P < 0.001$, Figure 4a). Histological staining of the affected synovial tissues demonstrated that administration of ZSTK474 (50 mg/kg) markedly attenuated infiltration of inflammatory cells, proliferation of synovial fibroblasts and cartilage/bone destruction (Figure 4b, Table 1). Especially, the number of OCs in talus decreased significantly in ZSTK474 (50 mg/kg)-treated group (Table 1). Furthermore, a remarkable reduction was observed in the arthritis score even in the therapeutic protocol in which ZSTK474 administration was begun (100 mg/kg) after development of arthritis. At Day 52, there were highly significant differences between the vehicle-treated group and the ZSTK474 (100 mg/kg)-treated group (mean arthritis score: 6.8 ± 1.0 versus 2.4 ± 0.5, Figure 4c). TRAP-staining of the joint section confirmed numerous OCs adjacent to the tarsal bones of vehicle-treated mice, whereas TRAP-positive OC formation in ZSTK474-treated mice was markedly decreased (Figure 5a). In addition, plasma levels of TRACP5b, a biomarker of systemic bone resorption, raised significantly in vehicle-treated, 25 mg/kg, and 50 mg/kg ZSTK474-treated mice, compared to intact mice. In contrast, the

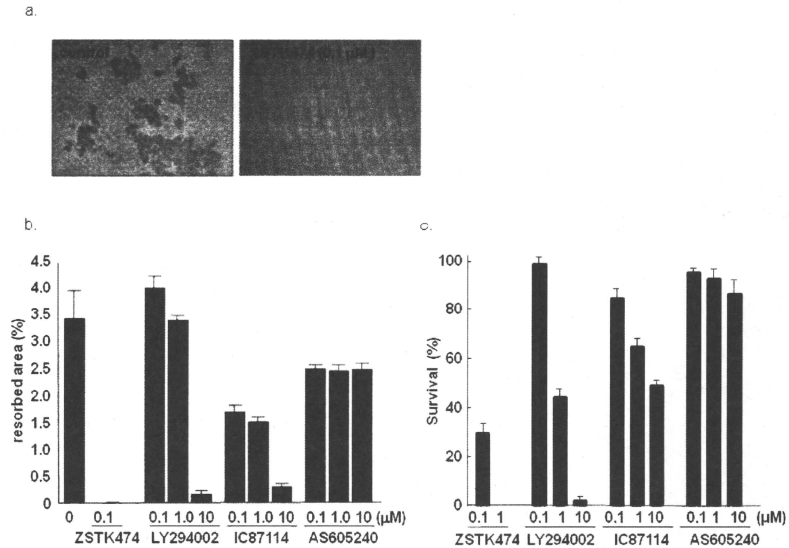

Figure 3 Blocking bone resorbing activity of OCs with ZSTK474. Mouse bone marrow derived monocytic OC precursors were co-cultured with osteoblasts in the presence of 1α,25-$(OH)_2D_3$ on a collagen gel-coated dish. The matured OCs were collected and transferred onto dentin slices and incubated for 72 hours in the presence or absence of ZSTK474 and other PI3-K inhibitors. The dentin slices were stained with hematoxylin, and the pits formed in the resorbed area on the slices were observed **(a)** and measured **(b)** under a light microscope. (**c**) Matured OCs, differentiated from bone marrow cells as described above, were further cultured with 5 ng/ml of TNF-α and the PI3-K inhibitors. After 24 hours, TRAP-positive multinucleated cells were counted, and the percentages of surviving cells were calculated. The columns and bars indicate the mean and S.D. from duplicated wells in **a)** and **c)**.

TRACP5b levels were sustained in 100 mg/kg ZSTK474-treated mice (Figure 5b).

Discussion

In this study, we demonstrated that ZSTK474, a novel PI3-K-specific inhibitor, suppressed osteoclastogenesis and bone resorption. The *in vitro* inhibitory effect of ZSTK474 on OC formation, observed by culturing bone marrow cells, was much stronger than that of LY294002. Although both inhibit all isoforms of class I PI3-K, the inhibitory activities of ZSTK474 (IC_{50}: PI3-Kα: 1.6×10^{-8} M; PI3-Kβ: 4.4×10^{-8} M; PI3-Kγ: 4.9×10^{-8} M; PI3-Kδ: 4.6×10^{-9} M) were much stronger than those of LY294002 (IC_{50}: PI3-Kα: 5.5×10^{-7} M; PI3-Kβ: 1.1×10^{-5} M; PI3-Kγ: 1.2×10^{-5} M; PI3-Kδ: 1.6×10^{-6} M) on all isoforms, especially PI3-Kδ [30]. A PI3-Kδ-selective inhibitor, IC87114 (1 μM), completely inhibited OC formation, while a PI3-Kγ-selective inhibitor, AS605240, had no inhibitory effect

Table 1: Histological score and osteoclast number

	Synovium	Leukocyte	Cartilage/bone	Osteoclast
Vehicle (n = 6)	2.3 ± 0.8	1.7 ± 0.9	2.7 ± 0.6	62.0 ± 38.6
ZSTK474 (n = 6, 50 mg/kg)	0.0 ± 0.0	0.0 ± 0.0	0.8 ± 0.3	0.3 ± 0.2
P-value	0.009	0.073	0.036	0.024

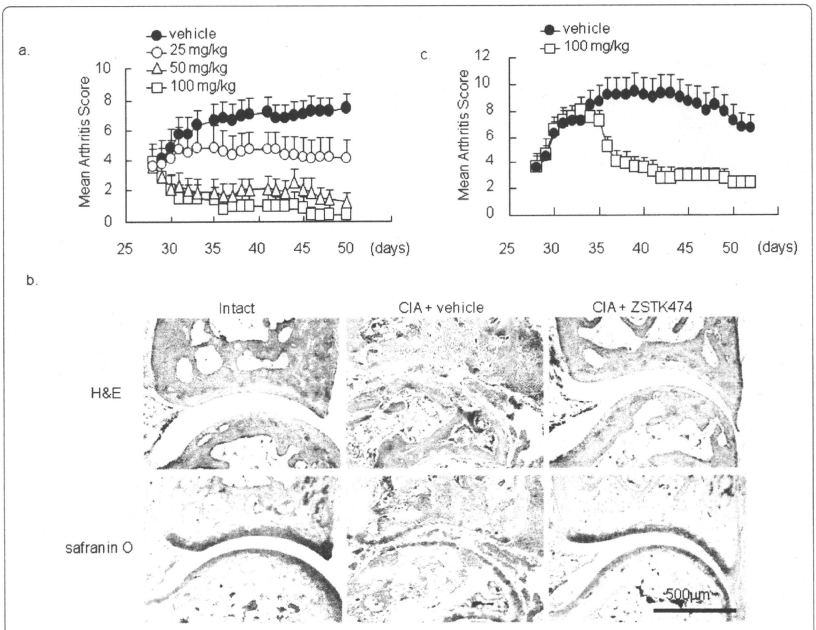

Figure 4 Oral administration of ZSTK474 ameliorated CIA in mice. *In vitro* effect of ZSTK474 was examined in mice CIA. On Day 28, when half of the mice had developed arthritis, oral administration of ZSTK474 was commenced once a day. **a)** Arthritis scores were compared among the groups. **b)** Synovial tissues from the hindpaws of vehicle-treated CIA mice, 50 mg ZSTK474-treated CIA mice and normal age-matched DBA mice were stained with hematoxylin and eosin (H&E) or with safranin O. Representative results are shown. **c)** In the therapeutic protocol, 100 mg/kg of ZSTK474 was started on Day 31, when all mice had developed arthritis.

on OC formation. These results indicate the involvement of PI3-Kδ in the OC culture system, consistent with a previous report which implicated a critical role of class IA PI3-K in OC formation by demonstrating that OC progenitor cells from mice lacking p85α, a regulatory subunit of class IA PI3-K, showed impaired growth and differentiation [23].

Blocking of the phosphorylation of Akt by ZSTK474 in RAW264.7 cells indicated that the inhibitory effect on OC formation observed in the bone marrow monocytic cells was due at least in part to suppression of PI3-K/Akt signal pathway in the OC precursors. This suggestion is supported by the observation that the consequent expression of NFATc1, an essential factor for terminal RANKL-induced differentiation of OCs [25,38], was also prevented by ZSTK474. The reduced expression of NFATc1 was dependent on neither NFkB nor cFos in the condition of this study. Additionally, translocation of NFATc1 into the nucleus was also inhibited by ZSTK474, implying that ZSTK474 might suppress the autoamplification, calcium-signal-mediated persistent activation [40], of NFATc1. Moreover, ZSTK474 inhibited the phosphorylation of Akt and OC differentiation induced by both RANKL and TNF-α, which are fundamental factors for OC formation in RA, implying that ZSTK474 might inhibit OC formation in patients with RA.

ZSTK474 also suppressed the bone resorbing activity of OCs as assessed in an *in vitro* pit formation assay. This could be explained by the inhibitory effect of ZSTK474 on survival of mature OCs in part. Likewise, signaling via PI3-K is crucial for remodeling and assembly of actin filaments, cell spreading and adhesion [41]. Furthermore, blocking PI3-K with ZSTK474 inhibited the membrane ruffling induced by platelet-derived growth factor